COMPUTER ANALYSIS OF NANOSCALE QUANTUM-DIMENSIONAL MODEL STRUCTURES IN EXTERNAL FIELDS

A.A. Gusev[a], O. Chuluunbaatar[a], V.P. Gerdt[a],
V.A. Rostovtsev[a], S.I. Vinitsky[b],
[a]Laboratory of Information Technologies and [b]Bogoliubov Laboratory of Theoretical Physics, Joint Institute for Nuclear Research
V.L. Derbov[c], V.V. Serov[c],
[c]Saratov State University, Saratov, Russia,
P.M. Krassovitskiy[d],
[d]Institute of Nuclear Physics, Almaty, Kazakhstan
and H.A. Sarkisyan[e],
[e]Russian-Armenian (Slavonic) University, Yerevan, Armenia

Problem

Spectral and optical characteristics of models of bulk semiconductor and low dimensional semiconductor nanostructures: quantum wells(QWs), quantum wires(QWrs) and quantum dots(QDs)

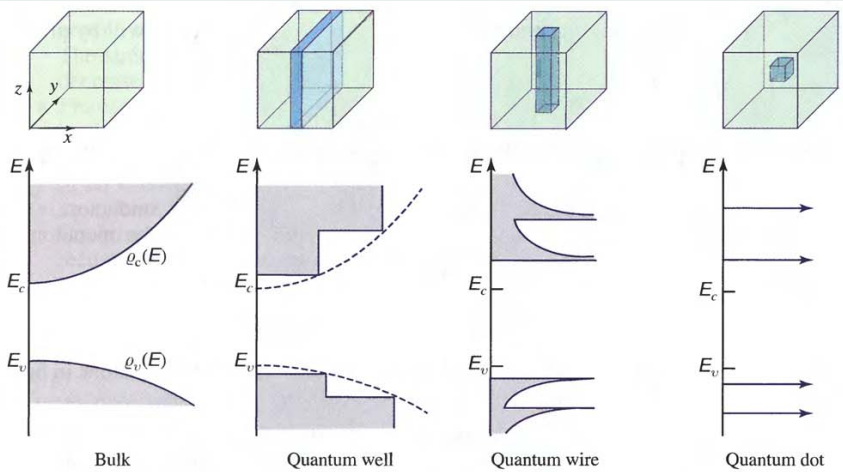

Figure 16.1-29 The density of states in different confinement configurations. The conduction and valence bands split into overlapping subbands that become successively narrower as the electron motion is restricted in a greater number of dimensions.

from B.E.A. Saleh M.C. Teich, Fundamentals of photonics (Wiley, 2007)

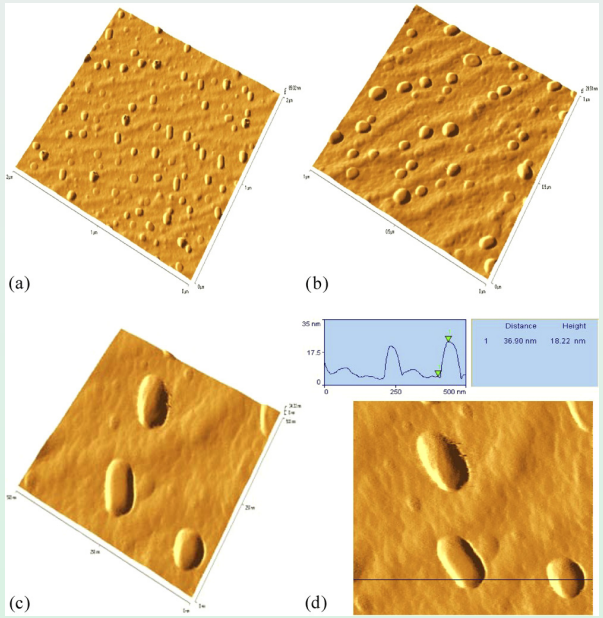

Figure 1. AFM views of LPE grown InAsSbP unencapsulated QDs on InAs(1 0 0) substrate: (*a*) oblique $S = 2 \times 2\,\mu\text{m}^2$, (*b*) oblique $S = 1 \times 1\,\mu\text{m}^2$, (*c*) oblique $S = 500 \times 500\,\text{nm}^2$ and (*d*) plane.

from K.M. Gambaryan et al J. Phys. D **41**, 162004 (2008)

Quantum Wells, Quantum Wires and Quantum Dots

Need for producing low dimensional structures => High performance transistors and lasers

Application of Quantum dots:
One of the most promising physical realizations of **qubits** is **singly charged quantum dot pair**:

Physical support	Name	Information support	$\|0>$	$\|1>$
Singly charged quantum dot pair	Electron localization	Charge	Electron on left dot	Electron on right dot

Superposition of $|0>$ and $|1>$ **qubit** states is **formed by external fields**.

Setting equations

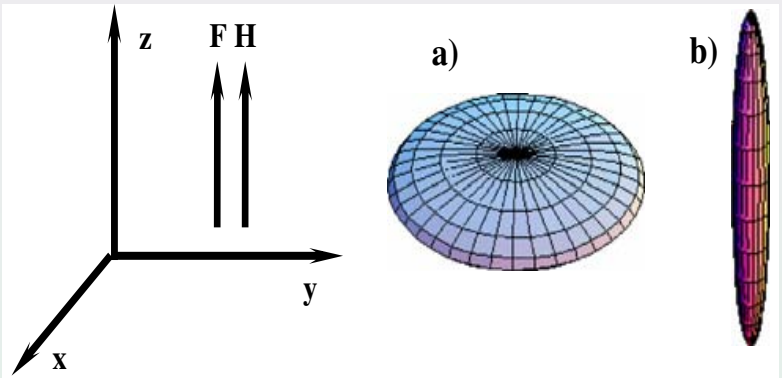

Fig. 1 (**a**) Strongly oblate ellipsoidal quantum dot. (**b**) Strongly prolate ellipsoidal quantum dot

In the effective mass approximation of the $\vec{k}\cdot\vec{p}$ theory the Schrödinger equation for the slow varying envelope function $\Psi(\vec{r}) \equiv \Psi^{e(h)}(\vec{r})$ of an impurity electron (e) or hole (h) under the influence of a uniform magnetic field $\vec{H}$ with vector-potential $\vec{A} = \frac{1}{2}\vec{H} \times \vec{r}$ and electric field $\vec{F}$ in QD, QW, or QWr reads as

$$\left\{ \frac{1}{2\mu}\left(\hat{\vec{p}} - \frac{q_1}{c}\vec{A}\right)^2 + (\vec{F}\cdot\vec{r}) + U_{conf}(\vec{r}) - \frac{q}{\kappa|\vec{r}|} - E \right\} \Psi(\vec{r}) = 0,$$

Here $\vec{r}$ is the radius-vector, $|\vec{r}| = \sqrt{x^2+y^2+z^2}$,
$q = q_1 q_2 e$, where $q_1 = \pm e$ and $q_2 e$ are the Coulomb charges of the electron (hole) and the impurity center, κ is the dc permittivity,
$U_{conf}(\vec{r})$ is infinite or finite (Woods-Saxon) well confinement potential
$\mu = \beta m_e$ is the effective mass of the electron or hole and reduced atomic units (for example, in GaAs $q = 1, \kappa = 13.18$, $\beta_e = 0,067, \beta_h = \beta_e/0.12$), $a_e = (\kappa/\beta_e)a_B = 102$Å, $E_e = (\beta_e/\kappa^2)Ry = 5.2$ meV, $a_h = 15$Å, $E_h = (\beta_h/\kappa^2)Ry = 49$ meV, $\gamma = H/H_0^*$, $H_0^* = 6$T).

Method

Reduction of elliptic boundary-value problems by:

1. exact solvable models
2. method of separation of variables
3. variational, Kantorovich and adiabatic methods
4. finite-element method
5. asymptotic method

Accuracy of calculation is 10 significant digits that corresponds to standard accuracy of laser spectroscopy.

Solution

We developed symbolic-numerical algorithms (SNA) and elaborated a problem-oriented complex of programs, now available via the Computer Physics Communication Library:

- ODPEVP: A program for computing eigenvalues and eigenfunctions and their first derivatives with respect to the parameter of the parametric self-adjoined Sturm-Liouville problem[1]
- POTHMF: A program for computing potential curves and matrix elements of the coupled adiabatic radial equations for a hydrogen-like atom in a homogeneous magnetic field[2]
- KANTBP & KANTBP 2.0: A program for computing energy levels, reaction matrix and radial wave functions in the coupled-channel hyperspherical adiabatic approach[3]

Downloaded 685 times.

---

[1] O. Chuluunbaatar, A.A. Gusev, S.I. Vinitsky and A.G. Abrashkevich, CPC 181, 1358-1375 (2009).

[2] O. Chuluunbaatar, A.A. Gusev, V.P. Gerdt, V.A. Rostovtsev, S.I. Vinitsky, A.G. Abrashkevich, M.S. Kaschiev and V.V. Serov, CPC 178, 301-330 (2008).

[3] O. Chuluunbaatar, A.A. Gusev, A.G. Abrashkevich, A. Amaya-Tapia, M.S. Kaschiev, S.Y. Larsen and S.I. Vinitsky, CPC 177, 649-675 (2007);
O. Chuluunbaatar, A.A. Gusev, S.I. Vinitsky and A.G. Abrashkevich, CPC 179, 685-693 (2008).

Models of QDs: Eigenfunctions

Oblate SQDs

Prolate SQDs

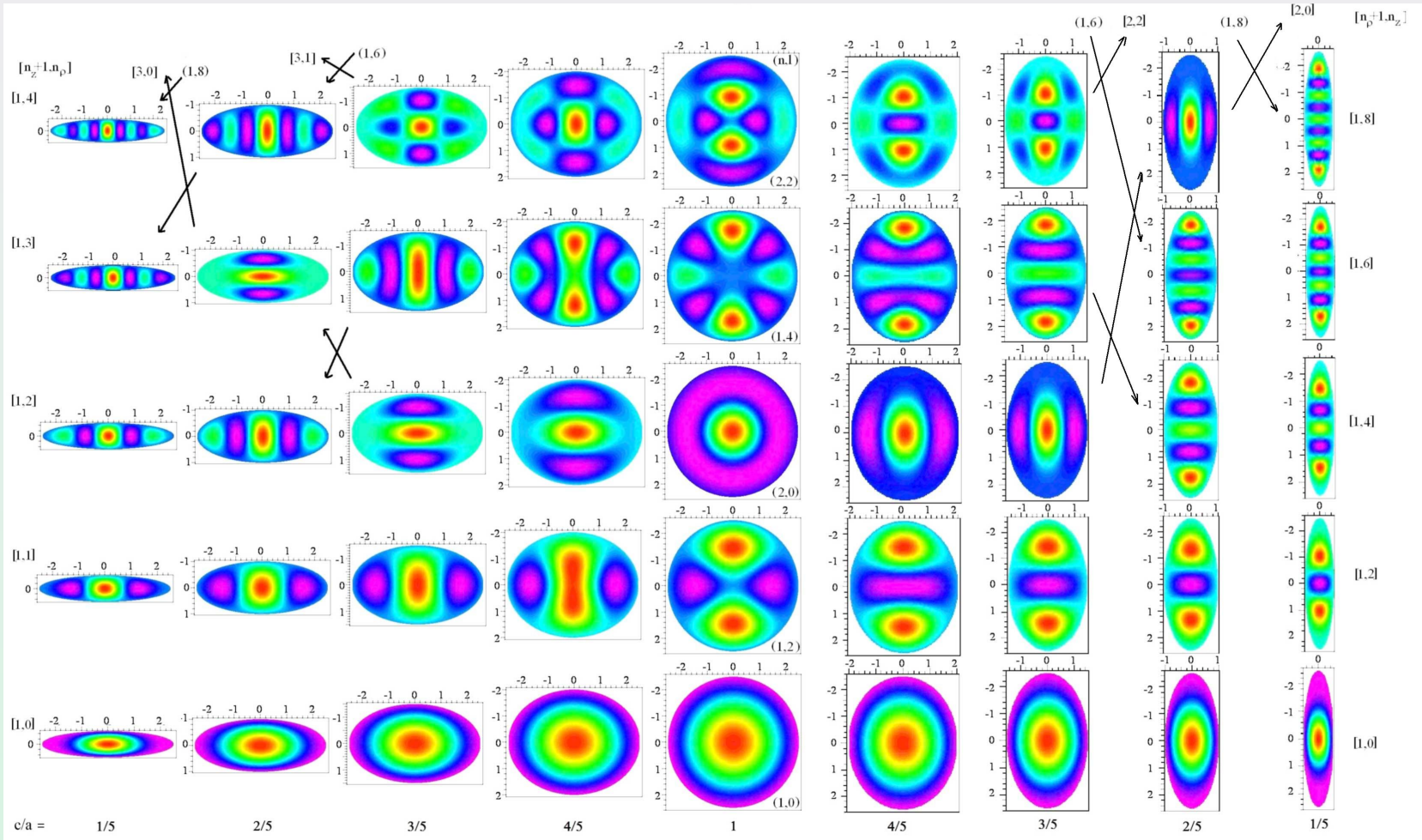

Contour lines of eigenfunctions in xz-plane for even electronic (hole) states of model spheroidal QDs versus the ratio c/a (or a/c) of minor c (or a) to major a (or c) semiaxis of the oblate (or prolate) spheroid.

Models of QDs: Energy levels

Oblate SQDs

Prolate SQDs

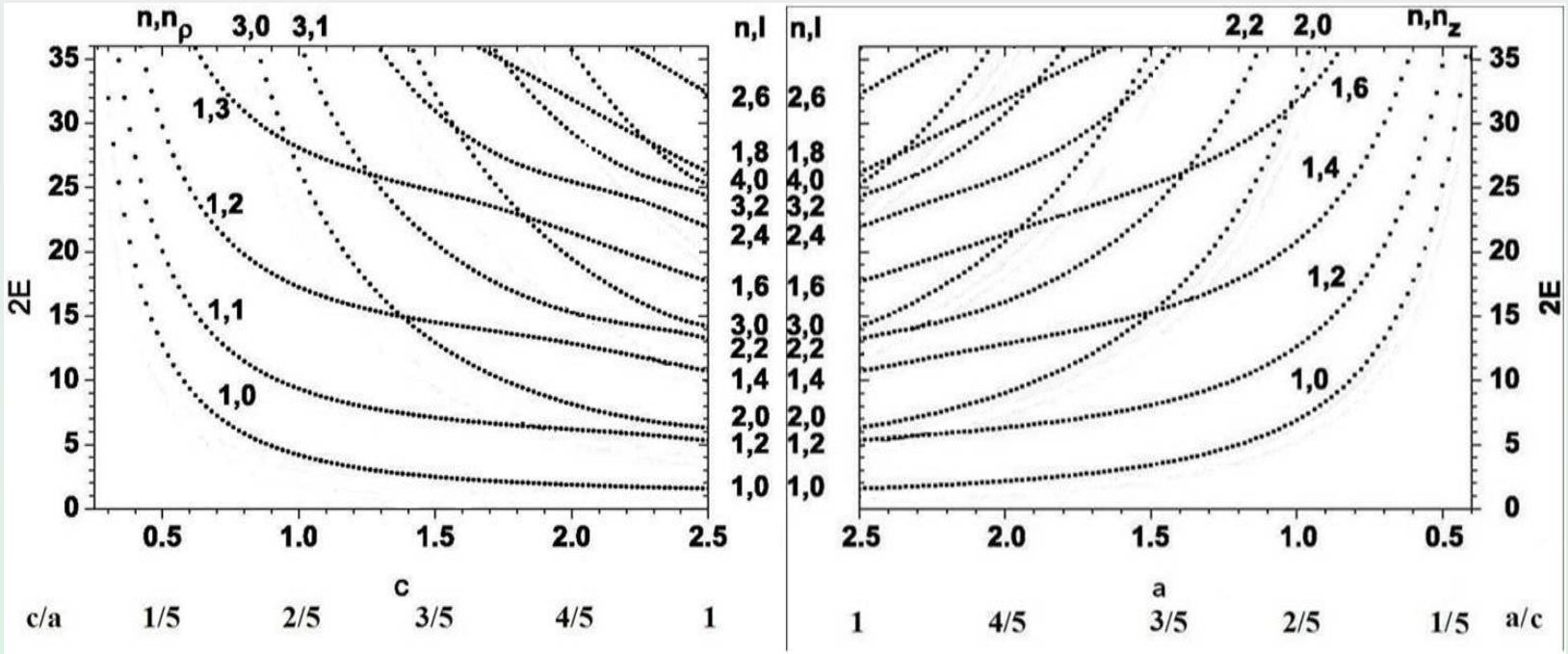

Energy levels (dotted lines) of even electronic (hole) states of model spheroidal QDs versus the ratio c/a (or a/c) of minor c (or a) to major a (or c) semiaxis of the oblate (or prolate) spheroid.

Models of QDs: Absorption coefficient

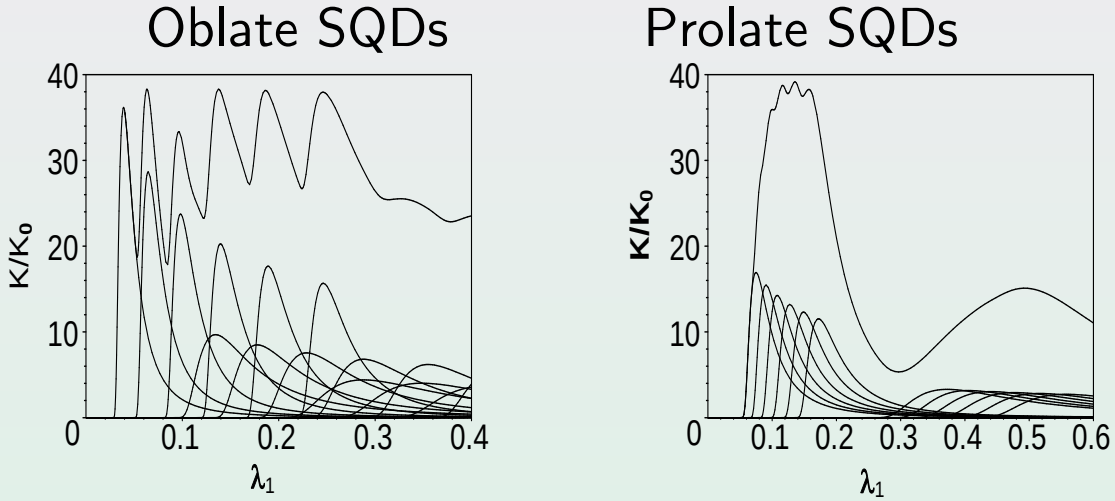

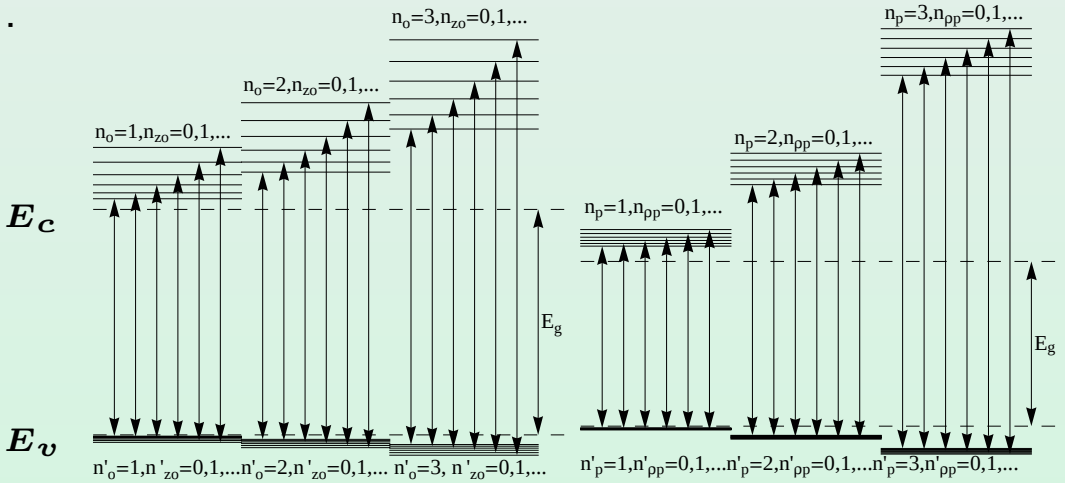

The absorption coefficient $\boldsymbol{K/K_0}$ for the ensembles of QDs, versus the energy $\boldsymbol{\lambda_1 = (\hbar\omega - E_g)/E_g}$ of the optic interband transitions for Lifshits-Slezov distribution of minor axis $\boldsymbol{\bar{c} = 0.5}$ at $\boldsymbol{a = 2.5}$ (or $\boldsymbol{\bar{a} = 0.5}$ at $\boldsymbol{c = 2.5}$).

The corresponding schematic diagrams of interband transitions.

Spectral characteristics of the prolate dumbbell QDs

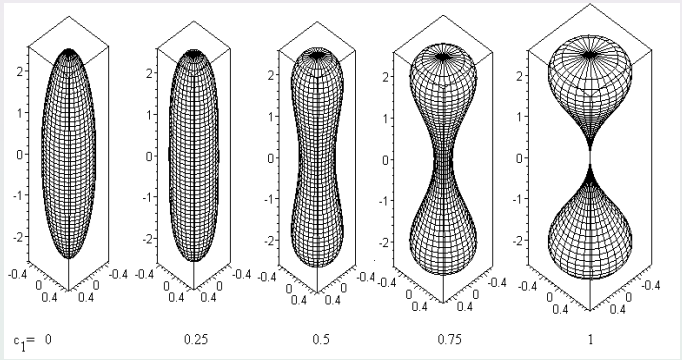

a)

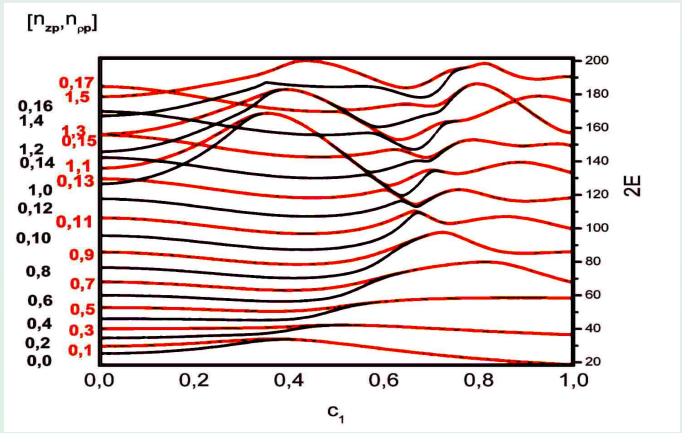

b)

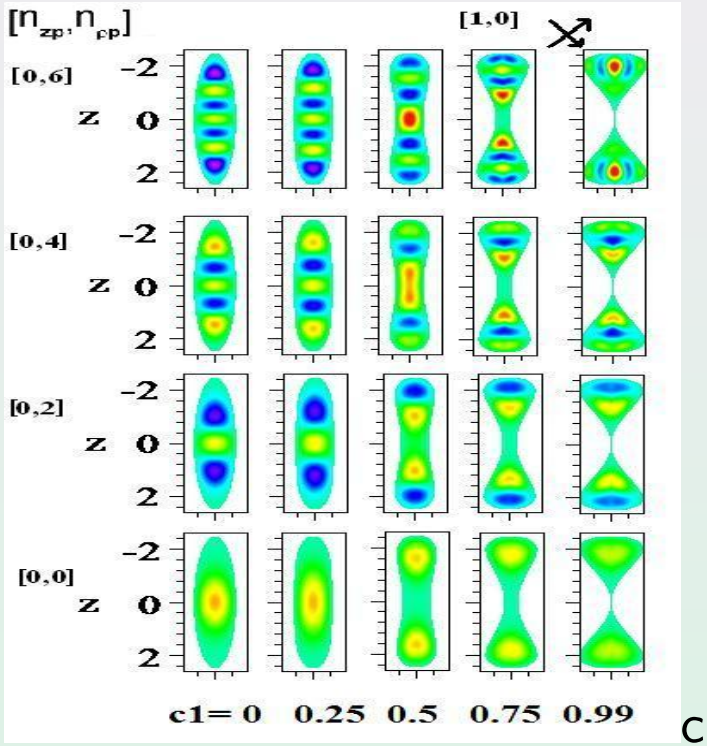

c)

a. The profile in plane xz of closed surface generated by rotating of continuous curve $\rho_0(z; a, c, c_1) = \frac{a}{c}\sqrt{c^2 - z^2}\,\frac{z^2 c_1^2 + 1 - c_1^2}{c_1^2 c^2/4 + 1 - c_1^2}$ about z-axis for $c = 2.5$, $a = 0.5$ vs $c_1 = 0, 0.25, 0.5, 0.75, 0.99$.

b. The energy levels of the **even** and **odd** electronic (hole) states for model B at $c = 2.5$, $a = 0.5$ vs c_1 classified at $c_1 = 0$ by cylindrical quantum numbers $n_{\rho p}, n_{zp}$ of PSQD.

c. Contour line of the first four even-parity wave functions in xz plane.

Models of QWrs: Axial changeling of similar charged ions

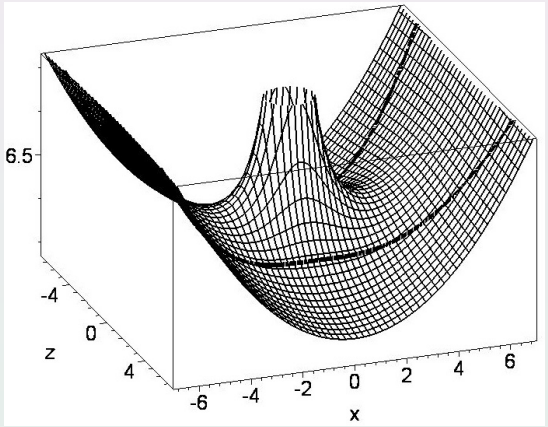

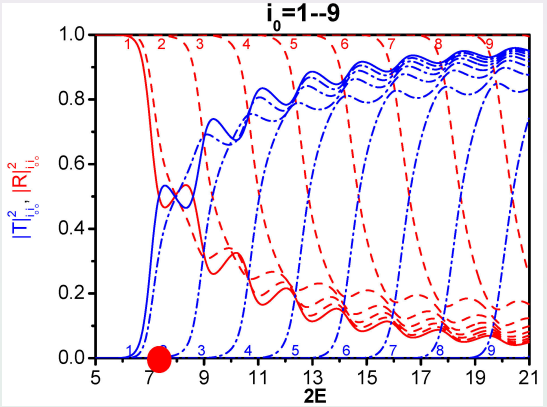

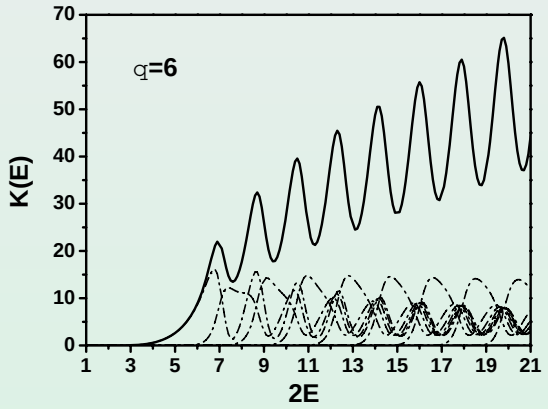

$|\Psi|$

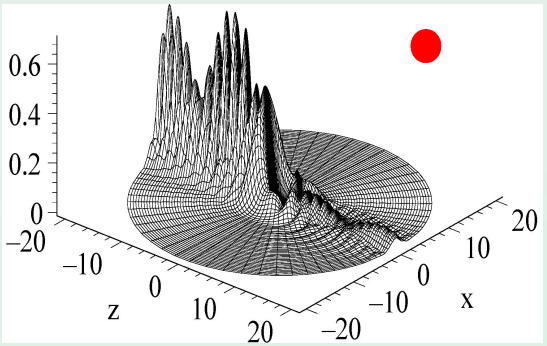

Diagonal elements of the transmission $|T|^2$ and reflection $|R|^2$ matrices, corresponding to the first nine open channels versus the energy $2E$ and enhancement coefficient $K = |\Psi(r = 0, \gamma)|^2/|\Psi(r = 0, \gamma = 0)|^2$ for the first component of the total wave function (solid line) and partial contributions (dash-dotted lines) of the open channels $i_o = 1 \div 10$, and wave function revealing resonance effects of total reflection and partial transmission with increasing collision energy.

Models of QWrs: Axial changeling of oppositive charged ions

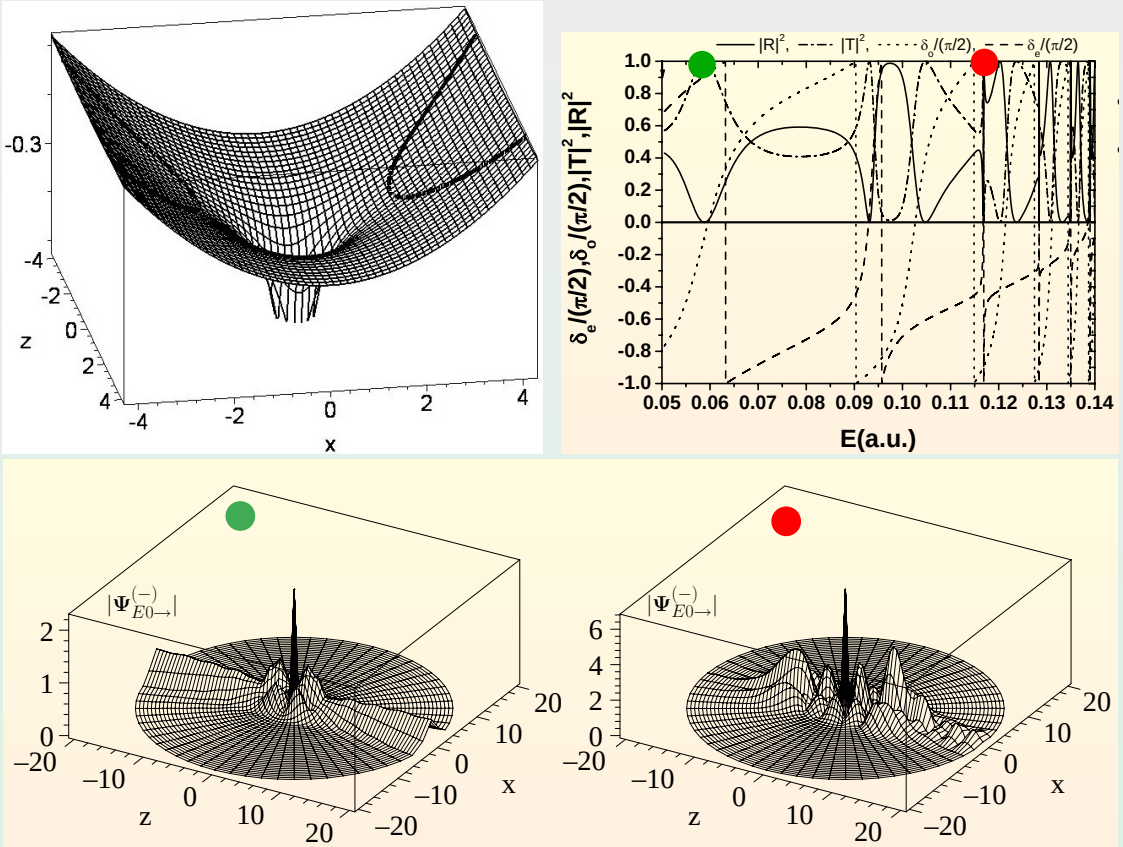

Transmission $|T|^2$ and reflection $|R|^2$ coefficients versus the energy E for continuum states of ion with charge $q = 1$ at $\gamma = 0.1$ and $m = 0$ between first and second thresholds and profiles of the continuum wave functions in xz-plane revealing resonance effects of the resonance transmission $|T|^2 = 1$ and total reflection $|R|^2 = 1$

Photoionization of hydrogen atom, exciton and impurity states of QWr in a uniform magnetic field

$$\sigma^d(\omega) = 4\pi^2 C\omega \times \sum_{i=1}^{N_o} |\langle \Psi_i^c(\mathrm{r})|z|\Psi^d(\mathrm{r})\rangle|^2,$$
$$\omega = E - E_d,$$
$$C \cong 0.20434 \times 10^{-22}\mathrm{m}^2$$

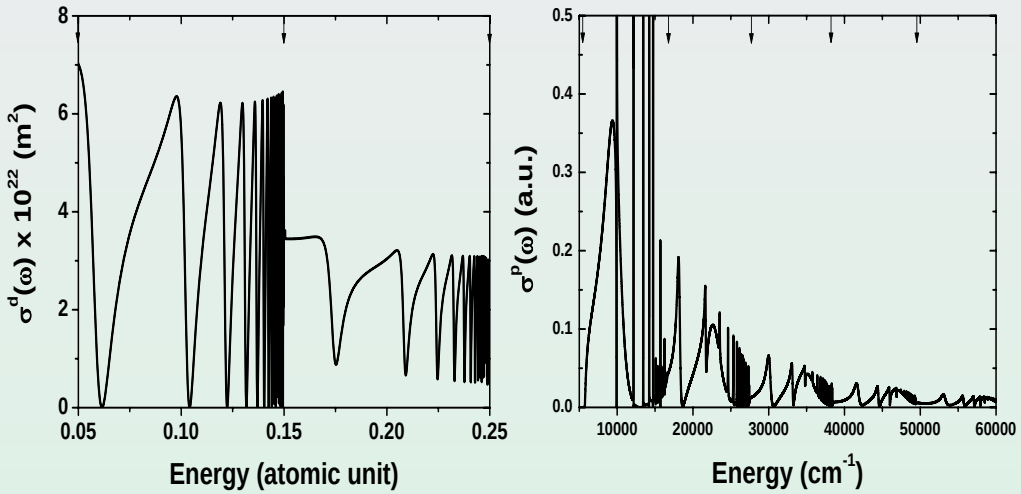

Photoionization cross-section $\sigma^d_{m\sigma\sigma'}(\omega)$ and $\sigma^p_{mm'\sigma}(\omega)$ vs energy E: (a) from the $1s_0$ state at $\gamma = 1 \times 10^{-1}$ ($H = 0.6$T for GaAs) into the final state $\sigma' = -1$, $m = 0$; (b) from the state $1p_{-1}$ at $\gamma = 5 \times 10^{-2}$ ($H = 0.3$T for GaAs) into the final state of continuous spectrum $m' = 0$. Arrows mark Landau thresholds $E_j = 1/2\epsilon^{th}_{mj} = ...$

Models of QWrs: recombination in magneto-optical traps

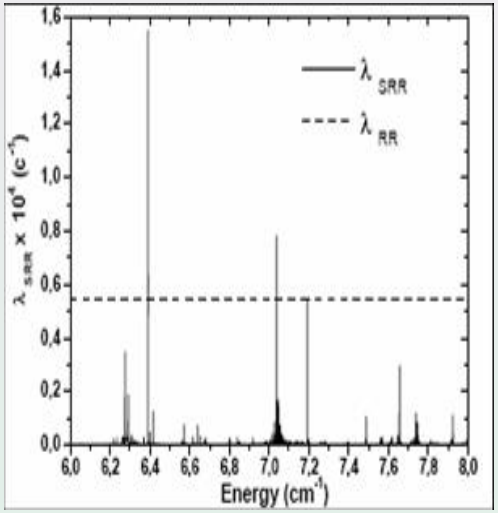

Laser-stimulated radiative recombination rate of positron and antiproton into the bound states $|N = 3, l = 0, m = 0\rangle$ in the magnetic field $H = 6$T and laser field with intensity $I = 24 W cm^{-2}$ at plasma temperature $T = 4$K and positron density $n_{e+} = 10^8 cm^{-3}$. The rate of the recombination into all nine states $N = 3$ for zero magnetic field $H = 0$ is shown by a dashed line.

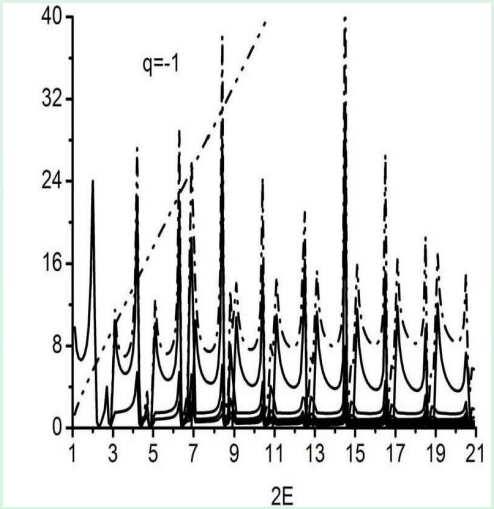

Enhancement absorption coefficient K/K_0 in resonance formation of exciton states belong to the continuous spectrum of GaAs valence band in the magnetic field $H = 6T$ vs the energy $2E$ at $m = 0$ (in reduced atomic units): for the first component of the total wave function (dash-dotted line), its approximate values (dash-dot-dotted line), and the partial contributions (solid lines) of the open channels $i_o = 1 \div 10$.

Quantum transparency of coupled pair of ions on barriers

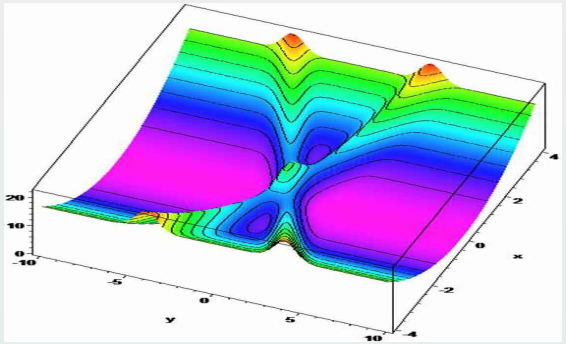

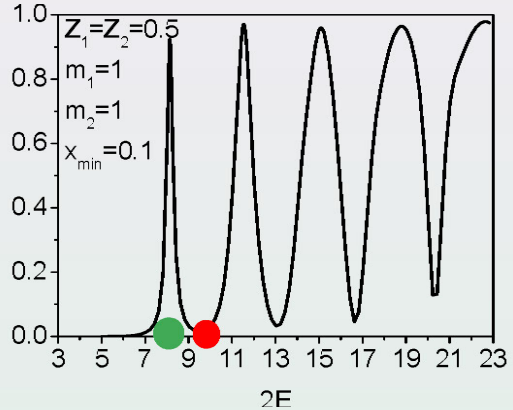

The total probabilities $T \equiv T_{11} = \sum_{j=1}^{N_o} |T_{1j}|^2$ of penetration through Coulomb-like repulsive potential barriers.

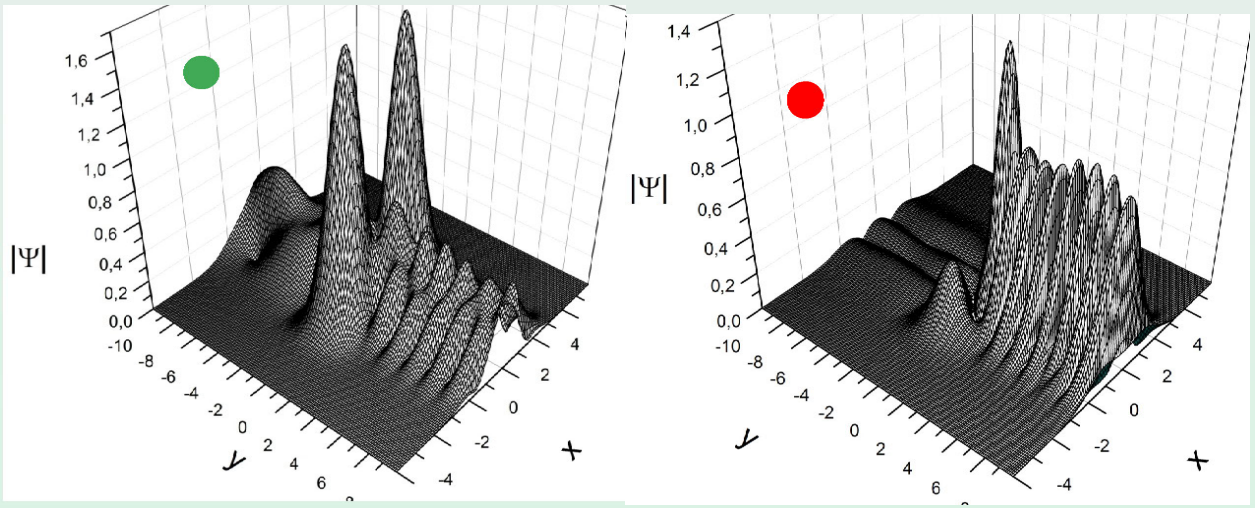

Profiles $|\Psi^{(-)}_{Em\rightarrow}|$ of the total wave functions of the continuous spectrum in the yx plane with $\hat{Z}_1 = \hat{Z}_2 = 0.5$, $m_1 = m_2 = 1$ at resonance energies $2E = 8.1403\, a.u.$ and $2E = 9.4748\, a.u.$, revealing *resonance transmission* or quantum transparency and *total reflection*.

Conclusion

The revealed difference in the spectra and the absorption coefficients allows verification of OSQD and PSQD models using the experimental data, e.g., photo-absorption coefficient and conductivity, from which not only the energy level spacing, but also the mean geometric dimensions of QDs can be estimated. The adiabatic approximations implemented in the analytic form can be applied also to treat a lower part of spectra of models of strongly deformed nuclei.

- Gusev A.A., Chuluunbaatar O., Gerdt V.P., Rostovtsev V.A., Vinitsky S.I., Derbov V.L., Serov V.V., Symbolic-Numeric Algorithms for Computer Analysis of Spheroidal Quantum Dot Models. Lect. Notes Comp. Sci. 6244, 106 (2010).
- Gusev A.A., Chuluunbaatar O., Vinitsky S.I., Dvoyan K.G., Kazaryan E.M., Sarkisyan H.A., Derbov V.L., Klombotskaya A.S., and Serov V.V., Adiabatic description of nonspherical quantum dot models. Phys. At. Nucl. (2012) (accepted); arXiv:1104.2292.

Conclusion

The revealed effects can be applied for preparing beams of atoms in prescribed Zeeman states and with required velocity projection onto the laser beam direction in high-precision spectroscopic experiments using laser-induced recombination in magneto-optical traps. The results are also important for the experimental study of low-energy nuclear reactions of channeling ions in thin films and crystals.

- Chuluunbaatar O., Gusev A.A., Vinitsky S.I., Derbov V.L., Melnikov L.A. , Serov V.V., Photoionization and recombination of a hydrogen atom in a magnetic field, Phys. Rev. A 77, 034702 (2008).
- Chuluunbaatar O., Gusev A.A., Derbov V.L., Krassovitskiy P.M., Vinitsky S.I., Channeling problem for charged particles produced by confining environment, Phys. At. Nucl. 72, 768 (2009).

Prospects

The computational scheme, the symbolic-numerical algorithms, and the complex of programs implemented in Maple–Fortran environment allow extension for the analysis of spectral and optical characteristics of the exciton states in finite-dimensional quantum models at the different geometry of structure, shape of confining potential, and external fields. They also look promising for developing quantum transparency and diffusion models, employment of MPI and Grid technologies.

Thank you for your attention !